*M. Lappa and L. Carotenuto*

# Effect of convective disturbances induced by g-jitter on the periodic precipitation of lysozyme

*Numerical simulations are carried out to investigate the crystallization process of a protein macromolecular substance under two different conditions: pure diffusive regime and microgravity conditions present on space laboratories. The configuration under investigation consists of a protein reactor and a salt chamber separated by an "interface". The interface is strictly related to the presence of agarose gel in one of the two chambers. Sedimentation and convection under normal gravity conditions are prevented by the use of gel in the protein chamber (pure diffusive regime). Under microgravity conditions periodic time-dependent accelerations (g-jitter) are taken into account. Novel mathematical models are introduced to simulate the complex phenomena related to protein nucleation and further precipitation (or resolution) according to the concentration distribution and in particular to simulate the motion of the crystals due to g-jitter in the microgravity environment. The numerical results show that gellified lysozyme (crystals "locked" on the matrix of agarose gel) precipitates to produce "spaced deposits". The crystal formation results modulated in time and in space (Liesegang patterns), due to the non-linear interplay among transport, crystal nucleation and growth. The propagation of the nucleation front is characterized by a wave-like behaviour. In microgravity conditions (without gel), g-jitter effects act modifying the phenomena with respect to the on ground gellified configuration. The role played by the direction of the applied sinusoidal acceleration with respect to the imposed concentration gradient (parallel or perpendicular) is investigated. It has a strong influence on the dynamic behaviour of the depletion zones and on the spatial distribution of the crystals. Accordingly the possibility to obtain better crystals for diffraction analyses is discussed.*

Mail address: Marcello Lappa
MARS Center, Via Gianturco 31 - 80146, Napoli, Italy
Fax: +39-81-6042100, E-mail: marlappa@marscenter.it
Paper submitted: 23.04.02
Submission of final revised version: 13.09.02
Paper accepted: 01.10.02

## 1. Introduction

Periodic precipitation is a generic term for material deposition processes which occur intermittently in terms of time or space or (generally) both. System dynamics depend on the interplay between transport in fluid phase and formation and growth of solid phases. These processes represent a special case of fashionable topic: oscillatory reactions, with practical implications in crystal growth and material preparation, and a theoretical kinship with the complex problems that come under the heading "order out of chaos". In the present paper the crystallization process of a protein substance (lysozyme) and the related "Liesegang Patterns" phenomena will be presented and analyzed under two different conditions: experiments carried out under pure diffusive regime and in presence of periodic accelerations typical of microgravity conditions.

Exploitation of microgravity environments in Physical Sciences (Fluid Science, Material Science) is motivated in most cases by the establishment of purely diffusive regimes (i.e. processes that take place in quiescent fluid media) that would prevail in an ideal (zero-g) environment. Typical experiments that would benefit of a quiescent or a quasi-quiescent condition are crystal growth experiments. These experiments are in fact characterized by mass transfer processes in fluid phases in presence of density gradients (caused by concentration gradients arising, for example, from the rejection or the incorporation of solute at a solid/liquid interface or by eventual temperature gradients imposed to drive crystallization). If gravity is present, these density gradients may be responsible of the onset of undesirable convection and sedimentation.

In the last years great interest has been directed towards crystals of biological macromolecules and in particular towards the crystallization process of protein substances under normal and microgravity conditions due to their relevance for progress in biotechnology and pharmaceutics. Typically these crystals are obtained by precipitation from super-saturated solutions with a number of techniques. For the case analyzed in the present paper, precipitation is induced by mutual diffusion of reagents and the related phenomenon is characterized by a certain degree of periodicity in time and/or in space. The term "periodic",

 

however, should be interpreted with caution and tolerance. Strictly speaking, it demands a period (i.e. a constant time or space interval), something that the phenomena here under discussion fail to show. These phenomena are nevertheless "periodic". The periods are not constant, but they are not random either. Periodic precipitations are often referred to as "Liesegang Patterns", because they were first studied by Liesegang. Liesegang patterns can manifest themselves in a great variety of media and ways.

On ground, typically investigators let reagents diffuse in some (preferably inert) environment. In this environment reagents react to produce "spaced deposits", each consisting of crystals. Under normal gravity conditions, sedimentation and convection, that would destroy the Liesegang patterns, are prevented by the use of gel. Agarose gel turns out to be a particularly suitable diffusion medium, because of its mechanical flexibility and chemical inertness. Due to its mechanical properties, crystals produced due to protein nucleation are "locked" on the matrix of agarose gel. If the gel matrix is not present, since crystals are denser than the feeding solution, sedimentation occurs and the crystals settle in the growth chamber.

With respect to these aspects, gel might represent a method to simulate microgravity on ground; however, it is not a real substitute of microgravity, because it might influence the crystallization process. The use of gel leads sometimes to detrimental effects in the quality of protein crystals obtained by periodic precipitation. On the other hand, the opportunity of accessing a low gravity environment in the last years to grow crystals of higher quality is still an open question. Buoyancy driven convection and sedimentation, the most important causes of imperfections and crystal defects are in fact reduced under microgravity conditions, but not suppressed. In addition, even if the residual gravity is reduced by several orders of magnitude in space, the presence of time-dependent accelerations (the so-called g-jitter disturbances: periodic accelerations of different amplitudes and frequencies) can induce convective motions. A large number of space experiments involving protein crystal growth have been carried out in recent years and many have offered conflicting results. Some of these experiments produced crystals that were larger and better ordered than the best ever grown on earth. For this reason the use of crystallization techniques under microgravity has been proved to be in principle a good candidate for growing crystals in a convection-free scenario. In spite of the perceived advantages of growing macromolecular crystals in space, however, there have also been a number of flight experiments that yielded crystals that exhibited no improvement in internal order, even for growth systems that had previously demonstrated significant improvements (Ramachandran, Baugher and Naumann [1]).

Such apparent scarce reproducibility could be explained according to the effect of g-jitters that (contrary to the case of steady g components) are specifically mission-dependent disturbances. Oscillatory g-jitter includes all the periodic time-dependent accelerations that can be approximated by sinusoidal functions. The most common sources of these disturbances are structural vibrations (e.g. at the fundamental natural frequencies), equipment operations and crew activity (e.g. repetitive exercises that induce cyclic displacement of the position of the growth reactor). For the reasons highlighted above, the understanding of the role of microgravity for protein crystal growth and its eventual benefit for obtaining high quality crystals are still open tasks and need further investigation. Particularly interesting is the interplay between nucleation and growth, on one side, and transport phenomena in fluid phase induced by

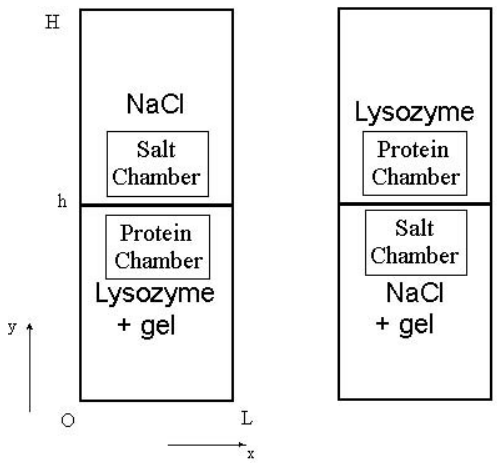


*Fig.1: Sketch of the configurations: (a) on ground configuration (b) microgravity configuration.*

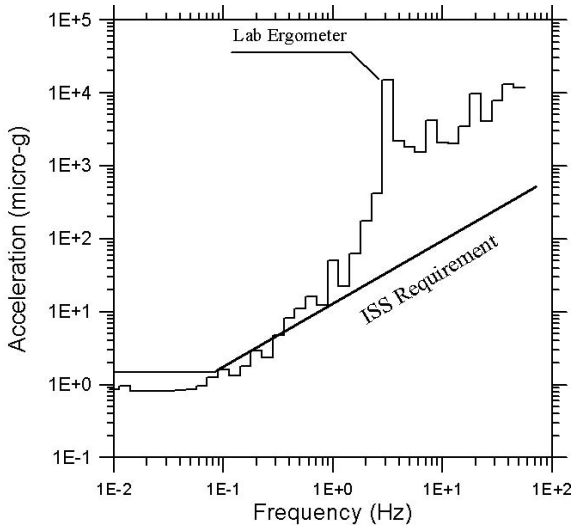


*Fig.2: Predicted high frequency g-jitter reported in a plot of acceleration amplitudes vs. frequencies and compared with the System Allowable (so called "ISS requirements curve").*

oscillatory accelerations, on the other hand.
While it is well known (see e.g. Qi and Wakayama [2]) that steady gravity levels may induce sedimentation of the freely suspended crystals and distortion of the concentration field, the role played by periodic accelerations in the dynamic process of periodic precipitation is still poorly understood. Recently the influence of these g-jitters on the dynamics of protein crystal growth in microgravity has been observed directly in the excellent analysis of Otàlora et al. [3]. They have reported novel results from micro-gravity-conducted experiments designed to monitor for the first time the development of the depletion zone around protein crystals and observing separately crystal and fluid motion due to g-jitter effects. The depletion zone around moving crystals under microgravity conditions was observed to be distorted by crystal movements induced by periodic accelerations.

Macromolecular crystallization is a matter of searching, as systematically as possible, the ranges of the individual parameters that impact upon crystal formation, finding a set or multiple sets of these factors that yield some kind of crystals, and then optimizing the variable sets to obtain the best possible crystals for X-ray analysis. For this reason most of the research efforts have been related to "what happen close to crystal". Many investigators have focused the attention on the behaviour of interfacial kinetics of nucleation and growth and on the morphology of the crystals (see e.g. Pusey et al. [4], Monaco and Rosenberger [5], Kuznetsov et al. [6], Coriell et al. [7]).

On the other hand, the present paper analyzes "ensemble behaviours", i.e. the macroscopic spatio-temporal evolution of the phenomena under investigation, with the objective of pointing out complex phenomenology. In fact, crystallization is characterised by the interplay of different processes: transport in liquid phase, nucleation and crystal growth. This global analysis may support the optimisation of growth techniques under normal gravity and in particular in space. The present numerical strategy can be seen as a very hybrid technique and considered an earliest example of a new class of volume of fraction methods (VOF) specifically developed for the case of organic growth from supersaturated solutions due to solubility modulation and the case of crystal motion, that has not appeared in literature until now.

## 2. Problem under investigation

### *2.1 Study configuration*

The configuration under investigation consists of a protein solution and a salt solution placed one above the other and separated by an "interface". The interface is strictly related to the presence of agarose gel in the lower solution (Figs.1). The protein is lysozyme (a well characterized model system) and the precipitant agent is NaCl salt (the system being at pH=4.5). The geometrical configuration is a chamber whose length and height are L and H respectively; the interface is placed at y≅ h. For the first case under investigation (diffusive regime) agarose is added to the protein solution in order to avoid crystal sedimentation and convection. The salt solution is located on the top of the protein solution (see Fig.1a). For the second case (microgravity conditions) the salt solution is filled with agarose gel; crystals produced in the protein chamber in this case are allowed to move according to the time-averaged velocity field due to g-jitter effects (see Fig.1b). At the initial time, both solutions are at constant concentration respectively. Experimentally, the shape of the gel interface cannot be horizontal due to the occurrence of a meniscus which is caused by surface tension effects. The function

$$\xi(x) = h\left\{1.1 - 0.1\left[\sin\left(\frac{\pi}{4} + \frac{\pi}{2}\frac{x}{L}\right) - \frac{\sqrt{2}}{2}\right] \Big/ \left(1 - \frac{\sqrt{2}}{2}\right)\right\}$$

is used to model interface curvature in order to have a minimum protruding in the lower chamber at the mean point along the horizontal length of the chamber ($\xi$ (x = 0) = $\xi$ (x = L) and the minimum at x = L / 2). The gel interface is supposed to be impermeable to the protein. The data used as input for the simulation are shown in Table 1.

### *2.2 Disturbances on the International Space Station*

Zero-gravity environments do not exist in the real world; all facilities for microgravity experimentation suffer from some degree of residual acceleration and g-jitters, arising mostly from orbiter manoeuvres. The expected disturbances on the International Space Station are:

1) Steady (or quasi-steady) residual-g. These include aerodynamic drag (1-3 $10^{-7}$ $g_o$), radiation pressure ($10^{-8}$ $g_o$), micrometeorites impacts ($10^{-9}$ $g_o$) and, for points distant from the center of mass, gravity gradient and rotation periodic with the orbit (O($10^{-7}$) $g_o$/[m]);

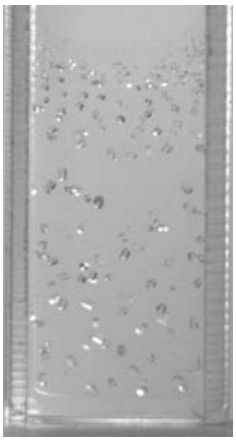

*Fig.3:*
*Experimental distribution of the crystals - (protein chamber filled with gel $C_{lys(o)}$=4 $10^{-2}$ [g/cm³]) Time=1.73 $10^5$ s*

2) periodic, high frequency, due to on board machineries and natural frequencies excited by external forces ($10^{-6} < g / g_o < 10^{-2}$, 0.1 [Hz] < f < 300 [Hz]).These deviations from true microgravity are known to be the origin of convective contribution to mass transport. The effect of steady (or quasi steady) residual-g of the order $O(10^{-6}\ g_o)$, however is not considered for the problem under investigation and is delayed to forthcoming analyses. Disturbances induced in a fluid cell by a sinusoidal displacement

$$\underline{s}(t) = b \sin(\omega t)\, \underline{n} \tag{1}$$

induce an acceleration:

$$\underline{g}(t) = \underline{g}_\omega \sin(\omega t) \tag{2}$$

where $\underline{g}_\omega = b\,\omega^2\,\underline{n}$ . The predicted high frequency g-jitter (e.g. recent NIRA 99 predictions for the US lab and for the ESA-COF) are usually reported in a plot of acceleration amplitudes vs. frequencies and compared with the System Allowable (so called "ISS requirements curve", see Fig. 2). Due to the large extension of the ISS and to the different vibrations induced by crew activities on the US Lab and on the ESA-COF module, the Space Station can be seen as an ensemble of microgravity platforms with substantial differences (in the convective disturbances) due to the different microgravity environments encountered by the experimental facility. In particular the recent NASA models predict a value of the residual-g of the order of 0.5 [μg] for the US Lab and of about 1.6 [μg] for the ESA-COF. On the other hand the g-jitter disturbances are expected to be larger in the US Lab than in the European COF. It is essential to recognize that the main difference between the US Lab and ESA COF is mainly due to the oscillation induced by the "Lab Ergometer" that is planned to be positioned inside the US Lab. In fact the amplitude, at a frequency close to 3 [Hz], induced by this equipment, is respectively about 150 [μg] for COF and 15000 [μg] for the US Lab (see Fig.2). The worst situation corresponding to the Lab Ergometer effect for the US Lab is considered in the present paper as reference case (worst conditions) to evaluate the effect of g-jitter disturbances on the lysozyme crystallization process. Two different cases are investigated: g-jitters disturbances perpendicular and parallel to the density gradient.

## 3. Mathematical model and numerical method

### *3.1 Growth in gel - Governing field equations*

The model is based on the mass balance equations, without consider cross-coupled coefficients, which are two order of magnitude lower at the considered concentration levels. Therefore, in absence of convection, the diffusion of lysozyme is governed by the equation

$$\frac{\partial C_{lys}}{\partial t} = \nabla^2 C_{lys} \tag{3}$$

A similar equation governs the diffusion of salt (in this case it is assumed that salt does not precipitate in solid phase). The non-dimensional form of the equations results from scaling the lengths by the horizontal distance between the walls (L), the time by $L^2/D_{lys}$, ($D_{lys}$ being the lower diffusion coefficient) and the concentrations of protein and salt by their initial values ($C_{lys(o)}$ and $C_{NaCl(o)}$). The walls and the gel interface are supposed to be impermeable to the protein.

### *3.2 Organic growth by solubility modulation*

In the case of organic substances, crystal growers usually obtain

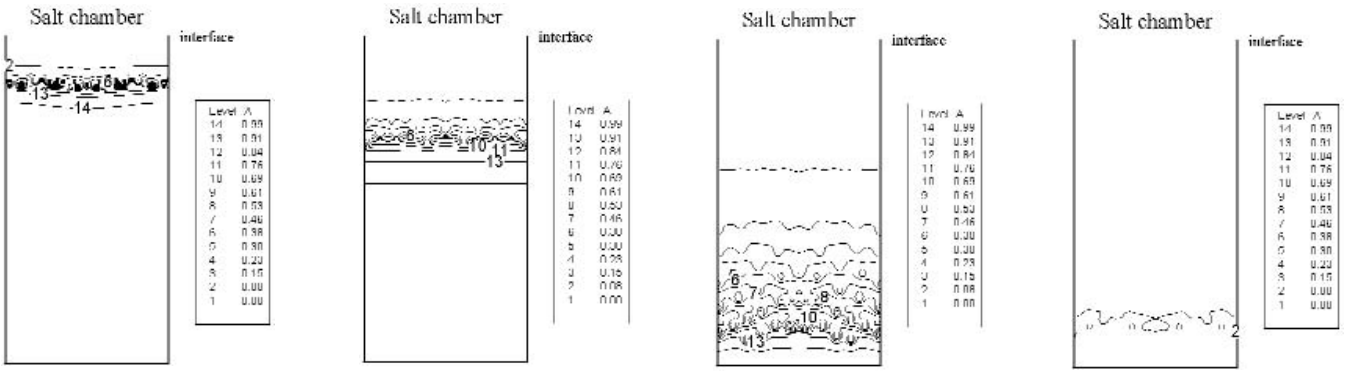


*Figs.4: Non-dimensional protein concentration contour lines (protein solution filled with agarose gel) Time=5.25 $10^3$ s (a), 2.625x$10^4$ s (b), 9.975 $10^4$ s (c), 1.73 $10^5$ s (d).*

deposition of material from solution by allowing a "reagent" to diffuse which does not actually react but acts modifying (reducing) the solubility (solubility modulation). Whenever protein in solute phase and solid crystal co-exist in equilibrium (saturation condition):

$$C_{lys} = S \tag{4}$$

where S is the solubility depending on the salt ([NaCl]) concentration. In a saturated solution, two states exist in equilibrium, the solid phase, and one consisting of molecules free in solution. At saturation, no net increase in the proportion of solid phase can accrue since it would be counterbalanced by an equivalent dissolution. Thus 'crystals do not grow from a saturated solution'. The system must be in a non-equilibrium, or supersaturated state to provide the thermodynamic driving force for crystallization.Solution must by some means be transformed or brought into the supersaturation state whereby its return to equilibrium, forces exclusion of solute molecules into the solid state, the crystal. As long as $C_{lys} < S$, more solid material will dissolve if any. If, on the other hand, $C_{lys} > S$, material will condense on any material already existing and augment its size. The 'growth regime' may be very complex and non-linear. The nucleation of new material is something else and the features of this phenomenon have to be modelled separately; the term 'precipitation' refers in fact to the composite phenomenon of nucleation and subsequent growth. Growth can take place at concentrations lower that those needed for nucleation, as long as $C_{lys} > S$. The solution is said to be *supersaturated* when the solute content is greater than S, and the degree of supersaturation $\sigma$ is defined by $\sigma = C_{lys} > S$. When there is no pre-existing deposit ([M]), it is generally found that the concentration of protein has to be greater than S to create one spontaneously, say $\sigma \geq \eta$ where $\eta$ is called the *"supersaturation limit"* (it is obvious that $\eta > 1$); once nuclei are created, precipitation can continue if $1 < \sigma \leq \eta$ and viceversa material can come back to the solute condition if $0 < \sigma < 1$. In this work it is assumed $\eta = 3$. The dependence of S of lysozyme on $C_{NaCl}$ has been determined experimentally (Otàlora and Garcìa Ruiz [8]).

*3.3 Discussion*

In the specific case of mass crystallization from a supersaturated solution one must generally accomplish at least two things simultaneously: (a) determine the concentration fields of organic substance and precipitant in the liquid phase and (b) determine the position of the interface between the solid and liquid phases. According to the technique used to address (a) and (b), in principle the numerical procedures able to solve these problems can be divided into different groups. If the size of the crystals is negligible with respect to the size of the reactor i.e. if the seeds are small and undergo only small dimensional changes with respect to the overall dimensions of the cell containing the feeding solution, the only information associated to each grain is its position and mass. These data can be stored in special arrays (three arrays are needed in this case: the first for the position along x, the second for the position along y and the third for the mass associated to each crystal). However a more elegant approach consists in introducing a non-dimensional phase-field variable $\phi$.

This approach accounts for the solid mass stored in the generic computational cell by assigning an appropriate value of $\phi$ to each mesh point ($\phi = 1$ computational cell filled with solid mass, $\phi = 0$ liquid and $0 < \phi < 1$ for a computational cell containing both liquid and solid phases). The key element for the method is its technique for adjourning $\phi$. Upon changing phase, the $\phi$-value of the cell containing the crystal is adjusted to account for mass release or absorption, this adjustment being reflected in the protein concentration distribution as either a source or sink. The modelling of these phenomena leads to the introduction of a group of equations. These equations are of algebraic type (Henisch and Garcìa Ruiz [9]) if the detailed description of the crystal surface morphology is not essential for the problem under investigation (present case) otherwise they

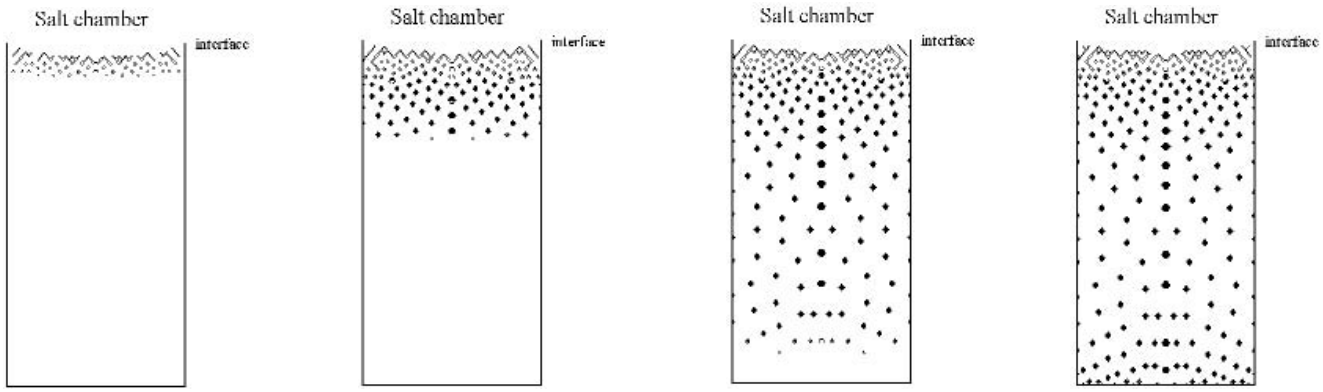


*Figs.5: Pattern of crystals (protein solution filled with agarose gel) Time=5.25 $10^3$ s (a), 2.625 $10^4$ s (b), 9.975 $10^4$ s (c), 1.73 $10^5$ s d).*

are differential equations associated to the attachment kinetics condition used to model mass transfer at the crystal surface (Pusey et al. [4]). The non-dimensional volume of the crystal mass M stored in a grid cell can be computed as ($\rho_P$ is the protein mass density in the crystal):

$$dv|_{stored} = \frac{1}{L^3}\frac{M}{\rho_P} \rightarrow \phi = \frac{dv|_{stored}}{dv} \qquad (6)$$

where dv is the volume of the computational cell.

*3.4 Nucleation and further precipitation*

*3.4.1. nucleation*

According to the crystallization criteria introduced by Henisch [10] (algebraic model), once the solid particles [M] are formed it is assumed that they are in equilibrium with protein and salt in liquid phase. Thus the concentration of protein has to satisfy eq. (4), i.e. the solute content of the solution will have to be decremented from the original $C_{lys}$ value to a value which must satisfy eq. (4).

If $\phi^m = 0$ and $\sigma^m = (C_{lys}/S)^m \geq \eta \rightarrow$

$(C_{lys})^{m+1} = S^m$, $M_{grain(0)} = (C_{lys} - S)^m C_{lys(o)} L^3 dv$,

$$\phi^{m+1} = \frac{1}{L^3}\frac{Mgrain(0)}{\rho P} = \frac{S^m Clys(0)}{\rho P}(\sigma - 1)^m \qquad (7)$$

these algebraic equations, where m superscript is used to indicate subsequent operations, model the nucleation process in a very simple way. We assume that the newly formed solid phase is constituted by only one crystal with mass $M_{grain(o)}$. Of course this assumption is not verified for very large values of supersaturation when an intense precipitation takes place, leading to a large concentration of nuclei. Typically, this occurs when supersaturation is increased very rapidly, with respect to the time needed for nuclei formation (induction time).

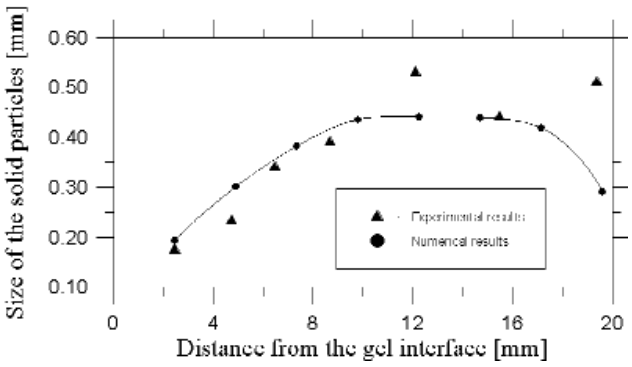


*Fig.6: Solid particle size distribution: comparison between numerical and experimental results (protein solution filled with agarose gel)*

The phenomena here under investigation are driven by the diffusion of salt through the gel interface. The nucleation process and further growth, in fact, are strictly associated to the modulation of the supersaturation limit and of the solubility due to salt diffusion. Therefore the characteristic time of the phenomena under investigation is the diffusion time of salt in the protein chamber ($t = h^2 / D_{NaCl} \cong 4 \cdot 10^5$s). The induction time according to Galkin and Vekilov [11] is of the order of $2 \cdot 10^3$ [s]. The relative importance of the two effects (characteristic induction time and characteristic diffusion time) is measured by the non-dimensional parameter:

$$\tau_{r.\,i.} = t_{induction} / t_{NaCl} \cong 5\ 10^{-3} \qquad (8)$$

Since $\tau$ is O ($10^{-3}$), the first effect can be neglected with respect to the latter. This explains why the increase of the supersaturation can be considered slow for the phenomena under investigation and at the same time allows the present mathematical-physical model to assume that if the supersaturation limit is exceeded, the amount of supersaturated protein in liquid phase becomes solid without any time delay (kinetic effects are negligible). By the technique under investigation a 'suitable' limited degree of supersaturation can be achieved. In very concentrated solutions, in fact, the macromolecules may aggregate as an amorphous precipitate. This result is to be avoided if possible and is indicative that supersaturation has proceeded too extensively or too swiftly.

*3.4.2. further growth or resolution*

In the presence of a deposit ($\phi > 0$), it is highly unlikely that the supersaturation will ever reach $\eta$ again, but if it is the case, secondary nucleation can occur, with formation of an additional deposit in the computational cell. However it is more likely that, due to salt transport in fluid phase, protein concentration becomes larger than S; in this case the existing deposit would grow; on the other hand, in case protein concentration becomes smaller than S, deposit would begin to re-dissolve. Two adjustable macroscopic "kinetic" coefficients $\beta$ ("re-solution coefficient") and $\alpha$ ("growth coefficient") are introduced to handle these phenomena (see Henisch [10]).

If $\phi^m > 0$ and $1 < \sigma^m < \eta \rightarrow$ further growth:

$$(C_{lys})^{m+1} = (C_{lys})^m - \alpha\,\delta_g,\ \ \delta_g = (C_{lys} - S)^m \qquad (9a)$$

$$M_{grain}^{m+1} = M_{grain}^{m} + \alpha\,\delta_g C_{lys(0)} L^3 dv,\quad \phi^{m+1} = \phi^m + \alpha\frac{S^m C_{lys(0)}}{\rho_P}(\sigma - 1)^m$$

If $\phi^m > 0$ and $\sigma^m < 1 \rightarrow$ resolution:

$$(C_{lys})^{m+1} = (C_{lys})^m + \beta\,\delta_i,\ \ \delta_i = (S - C_{lys})^m, \tag{9b}$$

$$M_{grain}^{m+1} = M_{grain}^{m} - \beta\,\delta i\, C_{lys(0)}\, L^3\, dv,\ \ \phi^{m+1} = \phi^m + \beta \frac{S^m C_{lys(0)}}{\rho_P}(\sigma - 1)^m$$

Kinetic effects may be relevant for large biological molecules, and they may influence growth and dissolution of deposits. To take into account this aspect two cases were considered:

a) $\alpha = \beta = 1$ (absence of kinetic effects);

b) $\beta = (M_{grain(o)} / M_{grain})^{1/3}$, $\alpha = 1 - 0.9\,(M_{grain(o)} / M_{grain})^{2/3}$.

The $\beta$ and $\alpha$ expressions in case (b) are introduced in Ref. [10] starting from two "well-known" behaviours: small grains dissolve more easily than large ones, large grains grow more rapidly than small ones. However, no relevant difference was observed from a macroscopic point of view between cases (a) and (b) for the conditions considered in the present simulations. For the present case of complex "periodic" phenomena (rhythmic dynamics) the macroscopic spatio-temporal evolution of the process is mainly driven by the availability of protein in liquid phase (many crystals compete for growth, the related depletion zones intersect and overlap) and by the rhythmic increase and decrease of supersaturation due to the interplay between protein depletion and salt diffusion through the gel interface. For this reason surface kinetics can be neglected while sacrificing little in accuracy for the macroscopic description of the spatio-temporal behaviour.

*3.5 Convection and g-jitter:*

The behaviour of fluid systems (e.g. fluid cells with temperature and/or concentration gradients) subject to sinusoidal accelerations has been the subject of intensive research in the last decade. Many theoretical and numerical studies have been dedicated to this topic (see e.g. Monti et al. [12], Mc Fadden and Coriell [13], Schneider and Straub [14], Alexander [15], Ramachandran [16], Monti and Savino [17]). It has been shown by an extensive numerical experimentation (Monti and Savino [18-20], Savino and Monti [21]) that convection arises when soliciting the fluid cell by periodic accelerations.

In particular, a number of computations for different study cases pointed out that the velocity field $\underline{V}$ induced by periodic $\underline{g}$ is made up by an average value $\overline{\underline{V}}$ plus a periodic oscillation of amplitude $\underline{V}'$ ($\underline{V} = \overline{\underline{V}} + \underline{V}'$). As a result of the convective field, the scalar quantities (species concentration) are distorted. These distortions are also made up by a steady plus an oscillatory contribution. Theoretical and numerical results available in literature pointed out that different situations may occur, depending on the oscillation frequency. It is well known (see e.g. [17-20]) that, increasing the frequency, there is a first regime characterized by relatively large oscillatory velocity and oscillatory concentration disturbances and relatively small time-averaged steady disturbances. On the contrary at high frequencies the oscillatory concentration disturbances are very small with respect to the steady ones induced by the time-averaged part of the velocity field. This behaviour suggested the investigators to introduce strong simplifications in the analysis of the disturbances computation. In particular, according to the Gershuni formulation (Gershuni, Zhukhovitskii and Yurkov [22]) the time-averaged distortions can be simply computed (i.e. with much less computation time) by a simplified set of equations in terms of quantities averaged over the oscillation period.

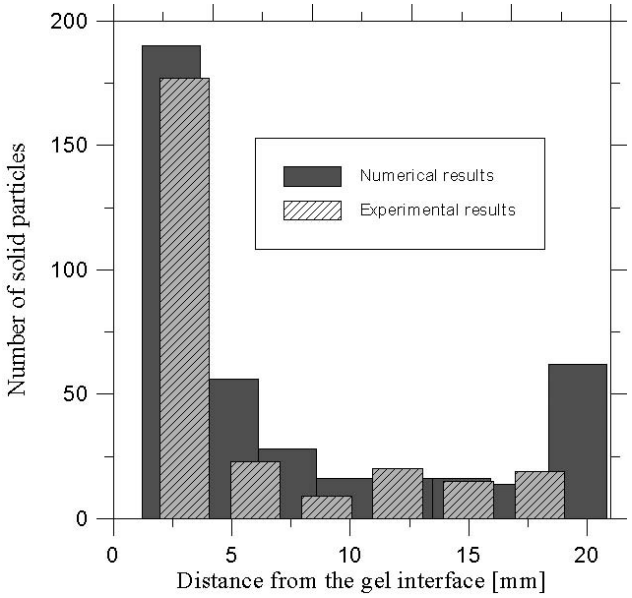


*Fig.7: Density of particles distribution: comparison between numerical and experimental results (protein solution filled with agarose gel)*

Simulations carried out by the different investigators in the case of simplified configurations used for fundamental research (e.g. test cells filled with model liquids) have shown moreover that the relative orientation of the imposed temperature or concentration gradients and of the direction of the periodic acceleration is a very sensitive parameter for the onset of convection and its intensity (according to these studies, the case of g-jitter disturbances perpendicular to the density gradient is expected to be the worst case whereas in the case of g-jitter disturbances parallel to the density gradient and in absence of precipitation phenomena, the effect of g-jitter should be always negligible). These aspects are here investigated in the case of periodic precipitation. For the present case, the flow is governed by the continuity, Navier-Stokes and species equations, that in non-dimensional conservative form read:

$$\nabla \cdot \underline{V} = 0 \tag{10}$$

$$\frac{\partial \underline{V}}{\partial t} = -\underline{\nabla} p - \underline{\nabla} \cdot [\underline{V}\,\underline{V}] + Sc\,\nabla^2 \underline{V} +$$

$$Sc \frac{b\,\omega^2\,\beta_{lys}\,L^3\,C_{lys(0)}}{\nu D_{lys}}\, C_{lys} \sin\left(\frac{L^2\omega}{D_{lys}} t\right)\underline{n} +$$

$$Sc \frac{b\,\omega^2\,\beta_{NaCl}\,L^3\,C_{NaCl(0)}}{\nu D_{lys}}\, C_{NaCl} \sin\left(\frac{L^2\omega}{D_{lys}} t\right)\underline{n} \qquad (11)$$

where b and ω are respectively the amplitude and the frequency of the oscillatory acceleration, V and p are the non-dimensional velocity and pressure and Sc = ν / $D_{lys}$. The reference velocity is $V_D = D_{lys}/L$ , the reference pressure is $\rho_{H_2O}\, D_{lys}^{\,2} / L^2$;

$$\frac{\partial C_{lys}}{\partial t} = -\underline{\nabla} \cdot [\underline{V} C_{lys}] + \nabla^2 C_{lys} \qquad (12)$$

$$\frac{\partial C_{NaCl}}{\partial t} = -\underline{\nabla} \cdot [\underline{V}\, C_{NaCl}] + D_{NaCl} / D_{lys}\, \nabla^2 C_{NaCl} \qquad (13)$$

The boundary conditions for $\underline{V}$ on the wall are the non-slip conditions. The nondimensional frequency (Ω) and displacement (Λ) can be defined by:

$$\Omega_{lys} = \frac{\omega L^2}{D_{lys}} \qquad (14a)$$

$$\Lambda_{lys} = b \frac{\beta_{lys}\, C_{lys(0)}}{L} \qquad (14b)$$

if based on lysozyme ($\beta_{lys}$ is the solutal expansion coefficient related to lysozyme) or by:

$$\Omega_{NaCl} = \frac{\omega L^2}{D_{NaCl}} \qquad (14c)$$

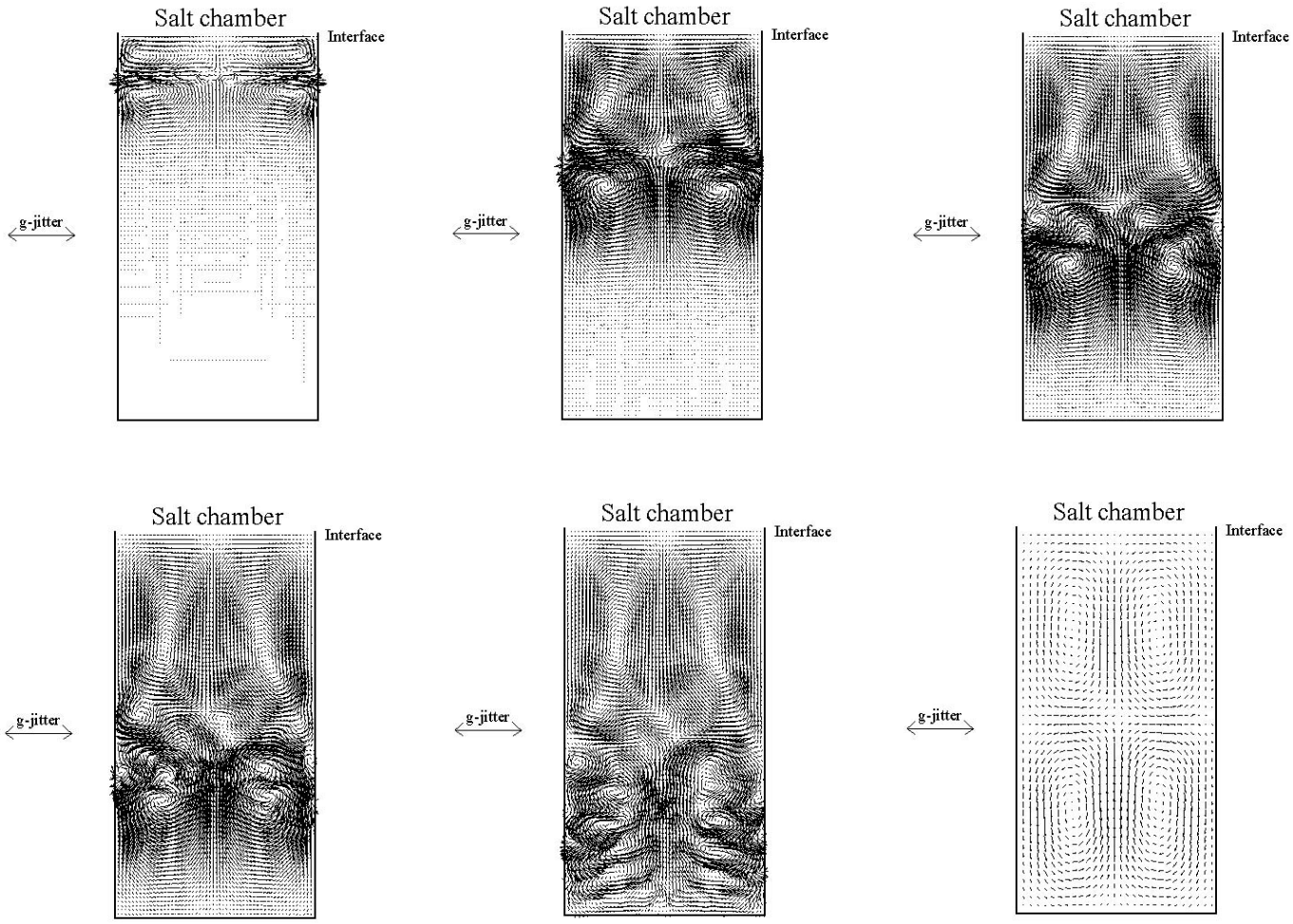


*Figs.8: Velocity field induced by g-jitter disturbances (microgravity conditions, worst case, Rav=$10^4$) Time=6.0 $10^3$ s (a), Time=2.6 $10^4$ s (b), Time=4.8 $10^4$ s (c), Time=6.8 $10^4$ s (d), Time=8.8 $10^4$ s (e), Time=1.7 $10^5$ s (f)*

$$\Lambda_{NaCl} = b\frac{\beta_{NaCl}\, C_{NaCl\,(0)}}{L} \tag{14d}$$

if based on salt ($\beta_{NaCl}$ is the solutal expansion coefficient related to salt). Under the assumptions of small amplitudes ($\Lambda << 1$) and large frequencies of the oscillatory accelerations ($\Omega >> 1$), the Gershuni formulation can be applied leading to a closed set of equations for the time-averaged quantities. The time-averaged continuity and species equations remain unchanged; the time-averaged momentum equation is written as:

$$\frac{\partial \underline{V}}{\partial t} = -\underline{\nabla} p - \underline{\nabla}\cdot[\underline{V}\,\underline{V}] + Sc\,\nabla^2\underline{V} + ScRav\left[\underline{w}\cdot\underline{\nabla}\left(C_{lys} + \frac{\beta_{NaCl}}{\beta_{lys}}C_{NaCl}\right)\underline{n} - \underline{w}\cdot\underline{\nabla}\,\underline{w}\right] \tag{15}$$

where

$$\underline{\nabla}\cdot\underline{w} = 0 \tag{16}$$

$$\underline{\nabla}\wedge\underline{w} = \underline{\nabla}\left(C_{lys} + \frac{\beta_{NaCl}}{\beta_{lys}}C_{NaCl}\right)\wedge\underline{n} \tag{17}$$

$\underline{n}$ is the unit vector associated to the direction of the g-jitter and Rav is the vibrational Rayleigh number

$$Rav = \frac{(b\,\omega\,\beta_{lys}\,LC_{lys(0)})^2}{\nu D_{lys}}$$

Eqs. (12-13 and 15-17) subjected to the initial and boundary conditions were solved numerically in primitive variables by a finite-difference method. The domain was discretized with a uniform mesh and the flow field variables defined over a staggered grid. Forward differences in time and central-differencing schemes in space (second order accurate) were used to discretize the partial differential equations. For further details on the numerical method see e.g. Savino and Monti [21] and Lappa [23].

*3.6 Crystal motion:*

Note that in the case of gellified phenomena the phase variable $\phi$ can be handled as an Eulerian variable (it is computed in the same points of the computational grid where the other quantities are evaluated) whereas in the case of crystal motion, $\phi$ behaves as a Lagrangian variable associated to marker particles and special arrays used to store its position and velocity. The phase variable $\phi$ is "transported" according to a Lagrangian equation solved for each of the solid crystals and its value is adjourned according to the algebraic equations of Henisch [10] modelling the release or absorption of protein. The concentration and velocity fields are updated according to an Eulerian description. For this reason the present strategy can be seen as a very hybrid technique and considered an earliest example of a new class of VOF methods specifically developed for the case of growth from supersaturated solutions due to solubility modulation and crystal motion. In the present paper the case of organic growth modelled by algebraic equations is investigated ("macroscopic" description of complex "periodic" phenomena (rhythmic dynamics)). The case of the detailed description of the "local" evolution (evaluation of the surface growth rate distribution for each crystal and shape morphology analysis) is out the scope of the present work and is delayed to forthcoming papers. In that case organic growth is governed by a set of differential equations (strictly associated to the surface incorporation kinetics) leading to the introduction of a different type of VOF method with respect to the one introduced here.

The viscous force acting on a solid particle (the crystals are assumed to be spheres) moving with a velocity $V_{grain}$ can be given in dimensional form (the overbar is used to highlight dimensional quantities) by Stokes law as

$$\overline{F}_D = 6\,\pi\,\overline{R}\,\mu\,\overline{\underline{V}}_{grain}$$

where $\mu$ is the coefficient of dynamic viscosity of the solution and $\overline{\underline{V}}_{grain}$ the velocity of the solid particle of radius R. The g-jitter force is given by

$$\frac{4}{3}\pi\,\overline{R}(\bar{t})^3(\rho_c - \rho_L)\,b\,\omega^2\sin(\omega\bar{t})\,\underline{n}$$

where $\rho_C$ and $\rho_L$ are the densities of the crystal and solution, respectively. The dimensional equation of motion of crystals reads:

$$\frac{4}{3}\rho_c\frac{d(\overline{R}(\bar{t})^3\overline{\underline{V}}_{grain})}{d\bar{t}} = \frac{4}{3}\pi\,\overline{R}(\bar{t})^3(\rho_c - \rho_L)\,b\,\omega^2\sin(\omega\bar{t})\,\underline{n} - 6\pi\,\overline{R}(\bar{t})\,\mu(\overline{\underline{V}}_{grain} - \overline{\underline{V}}) \tag{18}$$

i.e. it is assumed that, due to the small size of the moving crystals, the velocity field $\underline{V}$ is not affected by the motion of these particles and that, viceversa, the moving solid particles may be accelerated or decelerated by the effect of $\underline{V}$. In Eq. (18) ,

$$\rho_L = \rho_{H20}(1 + \beta_{lys}\overline{C}_{lys} + \beta_{NaCl}\,\overline{C}_{NaCl}),$$

$$R(t) = \frac{1}{L}\sqrt[3]{\frac{3}{4\pi}\frac{M_{grain}}{\rho_P}} = \sqrt[3]{\frac{3}{4\pi}\phi(t)\,dv}$$

and $M_{grain}(t)$ is the mass associated to each grain; note that the term

$$\frac{4}{3}\pi \bar{R}(\bar{t})^3(\rho_C-\rho_L)\,b\,\omega^2\sin(\omega\bar{t})\,\underline{n}$$

does not give average contribution to the motion of crystal (a solid particle under the effect of a high frequency sinusoidal acceleration simply moves forth and back around its position but its average location does not change) and for this reason it can be dropped. Eq. (18) in non-dimensional form reads:

$$\frac{d\underline{V}_{grain}}{dt}=-\frac{9}{2}Sc\frac{\rho_L}{\rho_C}\frac{\underline{V}_{grain}-\underline{V}}{R(t)^2}-3\frac{\underline{V}_{grain}}{R(t)}\frac{dR}{dt} \qquad (19)$$

which in discrete form reads (superscript n indicates time step):

$$\underline{V}_{grain}^{n+1}=\underline{V}_{grain}^{n}-\Delta t\frac{9}{2}Sc\frac{\rho_L}{\rho_c}\frac{\underline{V}_{grain}^{n+1}-\underline{V}^{n+1}}{(R^{n+1})^2}-3\frac{\underline{V}_{grain}^{n+1}}{R^{n+1}}(R^{n+1}-R^{n}) \qquad (20)$$

In eqs. (19) and (20) the dependence of the radius of the solid particle on the time has been highlighted in order to point out that the size of a moving particle may change due to further absorption (or release) of mass ($M_{grain}$ is a function of time) as explained in the previous sections. Eq. (20) has been solved for each crystal assuming:

$$V_{grain}=0,\quad x=x_{nucl},\ y=y_{nucl} \qquad (21)$$

where $(x_{nucl},y_{nucl})$ is the position at which nucleation occurs. Note that many simplifying assumptions have been introduced in the previous equations: the "apparent mass" of the crystals has been neglected and the viscous force has been computed according to the Stokes formula that is valid only at steady conditions (i.e. when the velocity does not change in time); these assumptions are supported by the fact that, for the conditions considered in the present work, the motion of the crystals is very slow (quasi-steady conditions).

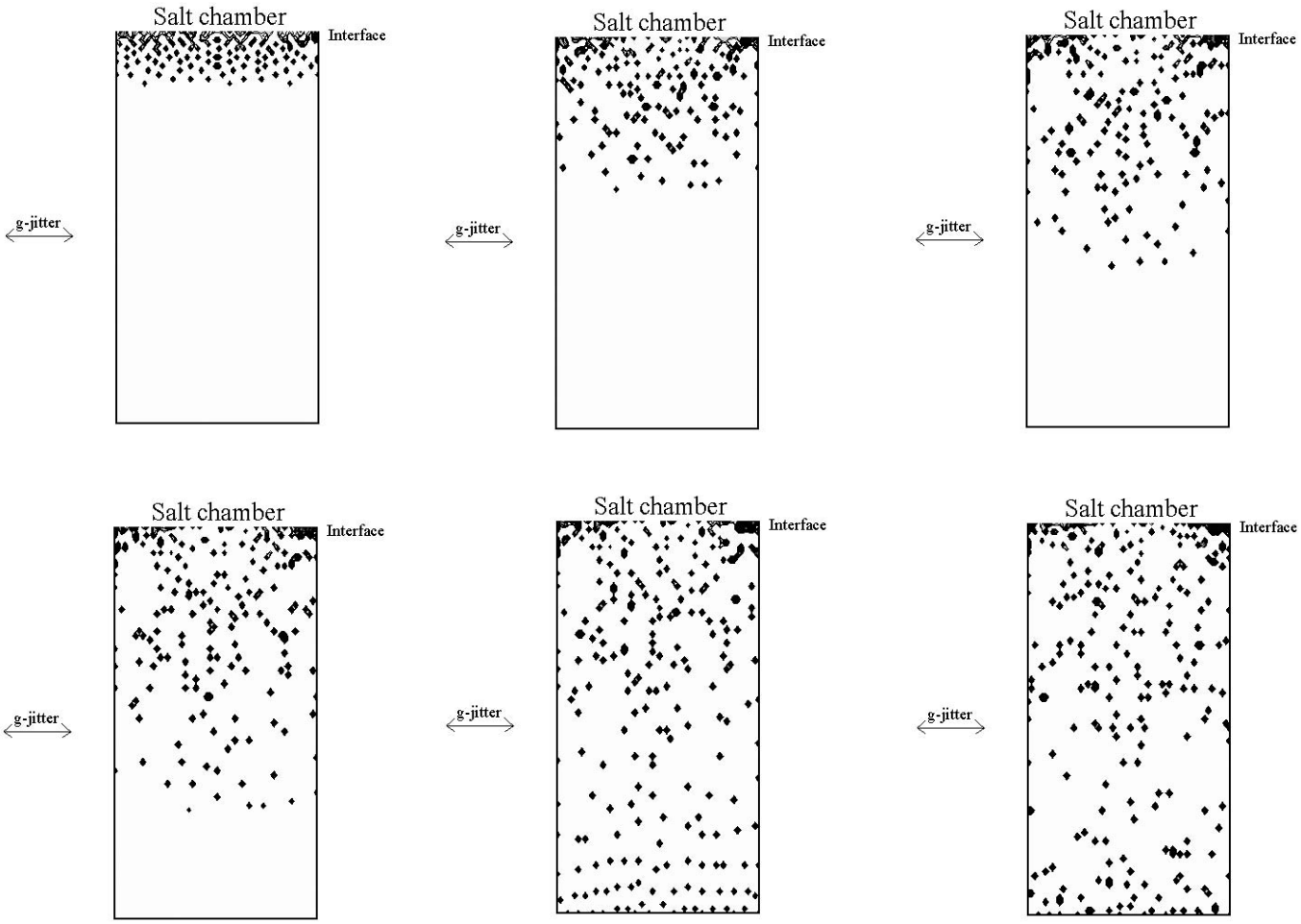


*Figs.9: Pattern of crystals (microgravity conditions, worst case, Rav=$10^4$) Time=6.0 $10^3$ s (a), Time=2.6 $10^4$ s (b), Time=4.8 $10^4$ s (c), Time=6.8 $10^4$ s (d), Time=8.8 $10^4$ s (e), Time=1.7 $10^5$ s (f).*

*3.7 Validation*

The numerical technique discussed from paragraphs 3.1 to 3.4 has been benchmarked against known and well documented numerical results. Validation has been obtained through several comparisons with the numerical simulations of Henisch [10]. The numerical method described in paragraph 3.5 requires the application of subroutines which have been already used by the authors in previous works and have been widely validated (see e.g. Ref. [21,23]). Finally, further validation has been provided by comparison with experimental observations.

**4. Results and discussion**

For the analysis of the periodic precipitation of lysozyme and the related formation of Liesegang patterns, the case of precipitation from a super-saturated solution with $C_{lys(o)} = 4 \cdot 10^{-2}$ [g/cm³] has been investigated.

*4.1 Periodic precipitation in gel (diffusive regime)*

The numerical simulations show, as expected and in good agreement with the experimental results (Fig.3 refers to experimental results described in Ref. [24], to be compared with Fig. 5d), that the phenomenon under investigation is characterized by a certain degree of periodicity in time and in space. Lysozyme precipitation produces deposits spaced in both the x and y directions (see Figs. 4-5). The "numerical" effect of a non-planar gel interface on the spatial distribution of crystals seems to be very important even if the deviation from the planar condition is very small (only 10 % of L, for further details on this topic, see e.g. Lappa et al. [25] where the sensitivity of the non-linear periodic precipitation to small asymmetries in the boundary conditions has been investigated in detail).

Figures (5a-d) show a two-dimensional displacement of the crystals. The bands of Liesegang patterns are not spatially uniform. Nucleating particles deplete their surroundings of protein which causes a drop in the local level of supersaturation such that the nucleation rate falls in the neighbourhood, leading naturally to a spacing between regions of nucleation that gives rise to the alternate presence of depleted zones and crystals. Fig.5a shows that after $5.25 \cdot 10^3$ [s], some crystals appear at the interface separating the protein chamber from the salt chamber. Correspondingly (see Fig. 4a) a "depletion zone" is visible around each solid particle. These zones with low concentration of protein are due to the fact that lysozyme concentration has been depleted to create the solid deposits. Due to the nucleation phenomenon described above, a "band", i.e. a region of low protein concentration, having a certain width is created all around the crystals. This band protrudes from the interface in the protein chamber and has a width somehow proportional to the amount of solid mass since the depletion of the protein concentration distribution is strictly related to the deposits created. The presence of solid particles near the interface can be explai-

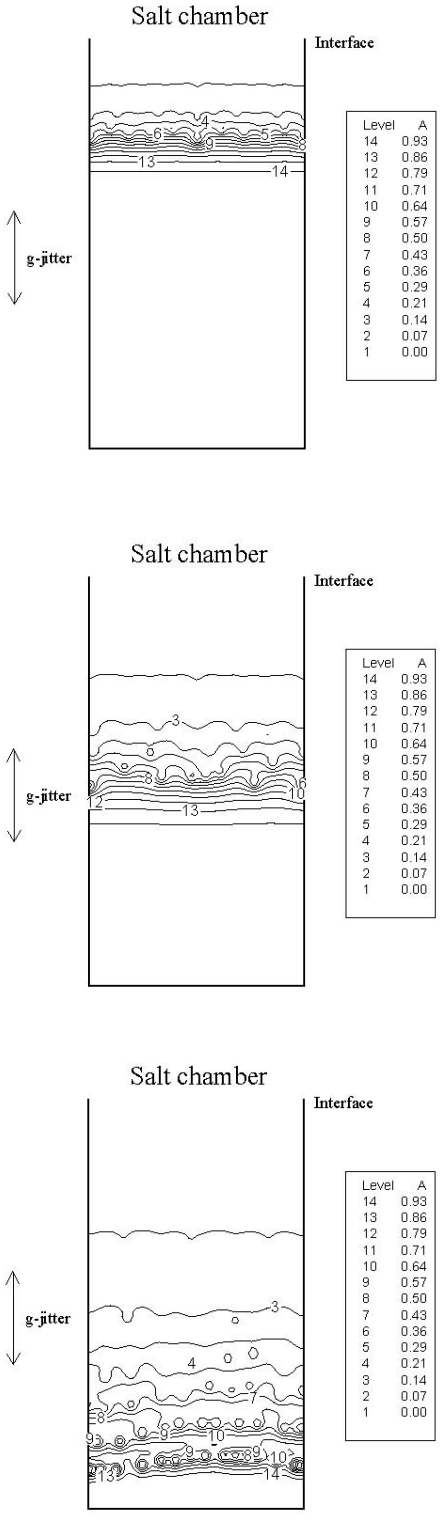


*Figs.10: Non-dimensional protein concentration contour lines (microgravity conditions, "ideal" case, Rav=$10^4$) Time=2.6 $10^4$ s (a), Time=7.4 $10^4$ s (b), Time=10.8 $10^4$ s (c).*

ned by the fact that salt diffuses in the protein chamber through the interface of gel so that solubility modulation first occur there. As time passes the size of these particles increase due to further precipitation of lysozyme. Figs. 4b and 5b show that even if no further nucleation occurs near the gel interface, solid deposits continue to grow thus increasing the extension of the "depleted band". The formation of the first nuclei depletes locally the protein solution; protein diffuses towards nuclei promoting their growth and enlarging the depletion zone. Therefore $C_{lys}$ is decreased and, even if salt diffuses downwards, lowering solubility further nucleation is prevented as far as $\sigma < \eta$. The increase of the solid particles size is due to the delicate balance between two counteracting effects: 1) protein condenses on any solid crystal already existing augmenting its size; this depletes the protein concentration and leads to lower values of $C_{lys}$ 2) salt continues to diffuse through the interface so that S is reduced due to solubility modulation. If the second effect prevails over the first one, i.e. the protein concentration is larger than the "solubility" then further protein precipitation in the considered region is possible.

As time passes the extension of the depleted zone increases towards the bottom of the protein chamber. This is due to the combined effect of the nucleation and precipitation phenomena. The propagation towards the bottom of the supersaturation front (i.e. the front where new nucleation occurs) depletes of lysozyme the protein chamber and further depletion occurs due to the phenomenon of subsequent precipitation. These two effects behave as a wave propagating towards the bottom (Figs. 4a-d). As time passes new regions are involved in the nucleation and further growth processes whereas previous regions are no longer characterized by these phenomena.

The spacing among different solid particles and the size of the particles seem to vary according to the distance from the origin of the imposed concentration gradient (for the present case the gel interface between the salt and protein chambers). The space distance among near solid particles, in fact, tends to decrease uniformly towards the interface of the protein chamber. Correspondingly the size of these particles (the size of the particles is computed modelling the solid particles as spheres of mass $M_{grain}$) is minimum at the interface and increases towards the bottom of the chamber up to a constant value in the bulk. The size then decreases again near the wall due to the effect of the solid boundary that does not allow solid particles to capture solute protein from the bottom. According to the results discussed above, the "density of particles" defined as ratio of the number of particles in a fixed reference volume and the reference volume, is maximum near the interface and almost constant in the bulk. These behaviours are shown in Figs. 6 and 7 where the numerical results are compared with available (see Ref. [24]) experimental ones. Comparison between experimental observation and numerical simulations provides further validation of the present mathematical model and gives insights on the crystallization process.

*4.2 Periodic precipitation under periodic gravity conditions*

Crystal growth under microgravity proceeds by the same chemical process as on ground, the only difference between them being fluid dynamics: mass transport is nominally diffusive in the gellified environment whereas, in absence of gel (microgravity conditions), concentration (density) gradients existing in the crystallizing solution (as elucidated in the previous paragraph) as an intrinsic consequence of the crystal-growth process may lead to the onset of convection. Regarding this aspect it should be pointed out that the benefits of crystal growth in microgravity conditions, can only be obtained if the crystals grow by addition of growth units supplied at a slow rate by mass transport through a stable depletion zone filtering the potentially disturbing protein or impurity concentration changes at the crystal surface (Otàlora et al. [3]). Therefore for microgravity

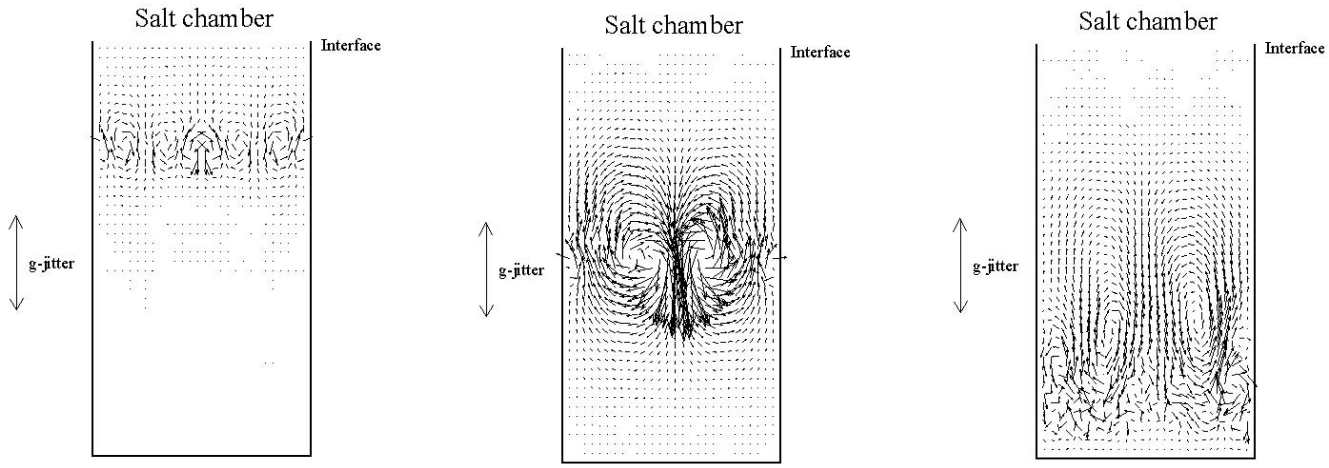


*Figs.11: Velocity field induced by g-jitter disturbances (microgravity conditions, "ideal" case, Rav=$10^4$) Time=2.6 $10^4$ s (a), Time=7.4 $10^4$ s (b), Time=10.8 $10^4$ s (c).*

experiments the definition of experimental conditions ensuring the development of stable depletion zones is a requirement as important as having a quiet diffusive environment. The present paragraph deals with the analysis of the phenomenon of lysozyme periodic precipitation (gel absent in the protein chamber) in presence of a high frequency sinusoidal acceleration (corresponding to the US-Lab Lab Ergometer conditions, i.e. f = 3 [Hz], $g = b\omega^2 \cong 1.5\ 10^4$ [μg], Rav ≅104). The non-dimensional frequency and amplitude associated to the Lab Ergometer conditions in Fig.2 are respectively $\Omega_{lys} \cong 2 \cdot 10^7$, $\Lambda_{lys} \cong 5 \cdot 10^{-4}$ and $\Omega_{NaCl} \cong 2 \cdot 10^6$, $\Lambda_{NaCl} \cong 3.5 \cdot 10^{-3}$ i.e. the present case falls with good approximation within the range of validity of the Gershuni formulation.Two different cases are considered: g-jitters disturbances perpendicular to the imposed salt and protein concentration gradients (g-jitter parallel to the x axis, worst condition) and parallel to the concentration gradients (g-jitter parallel to the y axis, "ideal" condition). The comparison between these results and those described in the previous paragraph gives insight into the effect of g-jitter residual accelerations on the phenomena under microgravity conditions. First we focus the attention on the worst case, then the ideal condition is discussed and compared with the worst one.

For the first case, the results show that, due to density gradients associated to salt diffusion and protein depletion occurring in the protein chamber, convection cells arise (velocity is of the order $O(10^{-6}$ [cm/s]). The flow organization is very complex since multicellular structures are formed. Four main vortex cells are visible in the protein chamber. These vortices have the classical Gershuni configuration (see e.g. [21]), i.e. two couples of counter-rotating vortex cells (each couple formed by two convection rolls mirror-symmetric with respect to the position x=L/2, see Figs. 8a-c). Figs. 8a-c show that at each instant the line of separation between the two couples of convection cells corresponds (approximately) to the position of the nucleation front (see Figs.9). As time passes the nucleation front and the line of separation migrate increasing their distance from the gel interface.According to this behaviour, the region where solid particles are present (region between the gel interface and the nucleation front) is affected by the presence of two counter-rotating vortex cells located on the right and on the left of the position x=L/2 respectively. Solid particles are transported towards the gel interface near the walls (x=0 and x=L) and in opposite direction around x=L/2. Crystals located around x=L/2 leave regions where protein has been depleted and are transported towards regions where the amount of protein available in liquid phase is still large. On the opposite, crystals located near the walls are transported towards regions where the protein has been reduced due to previous nucleation and further growth

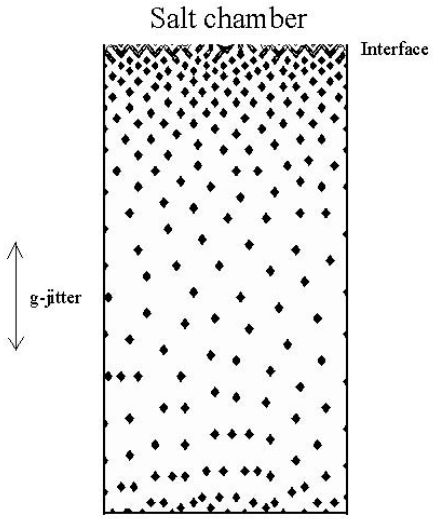


*Fig.12: Pattern of crystals - (microgravity conditions,"ideal" case, Rav=$10^4$) Time=1.7 $10^5$ s*

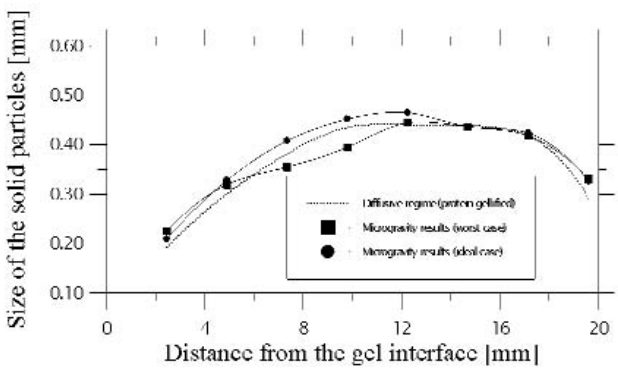


*Fig.13: Solid particle size distribution: comparison between pure diffusive regime (gellified configuration) and microgravity conditions (g-jitter disturbance)*

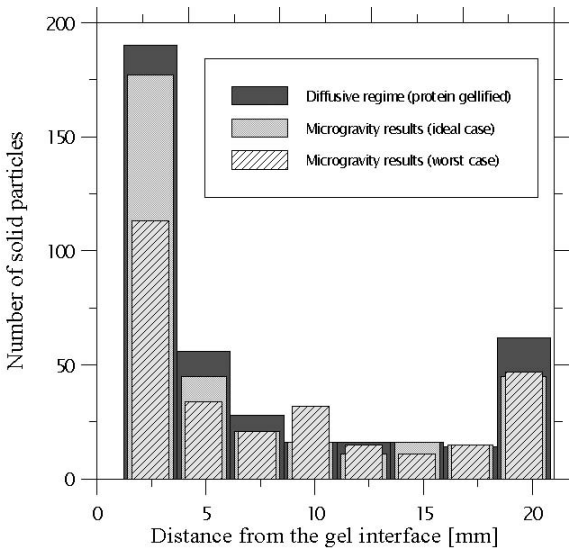


*Fig.14: Density of particles distribution: comparison between pure diffusive regime (gellified configuration) and microgravity conditions (g-jitter disturbance)*

phenomena. For these reasons crystals located around the mid-section have larger size with respect to crystals located near the walls (they in fact take advantage of the larger amount of protein available with respect to their initial position and viceversa for the crystals located near the walls).

As time passes, the velocity field becomes very complex (Figs.8d-8f). According to this behaviour the patterns of crystals are no longer characterized by the somehow repetitive structure and configuration observed in the previous paragraph. The distribution of the crystals in fact tends to be chaotic and irregular (compare e.g. Fig. 5d and 9f). This behaviour shows the "high sensitivity" of the system to the effect of the g-jitter. The deviation of the crystal distribution from the diffusive one may be considered a measure of the effect of the g-jitter disturbances on the complex rhythmic dynamics driven by the availability of protein in liquid phase and by the rhythmic increase and decrease of supersaturation due to the interplay between protein depletion and salt diffusion through the gel interface.

For the "ideal" case (g-jitter parallel to the y axis) in absence of nucleation phenomena (purely "diffusive" conditions), no vortex cells should arise since it is well known (see e.g. Ref. [21]) that concentration (and/or temperature) gradients parallel to the direction of the sinusoidal acceleration do not contribute to the onset of convection. However due to nucleation phenomena and further growth, concentration gradients perpendicular to the g-jitter direction are created leading locally to the onset of vortices (velocity is of the order O($10^{-6}$ [cm/s] as for the worst case). This is shown in Figs.11a-c. The presence of vortex cells is strictly confined to the zones where new nucleation and/or further precipitation occurs (i.e. around the nucleation front, see Figs. 10a-c). The region affected by multicellular convective structures migrates with the nucleation front whereas the remaining part of the protein chamber is free of convection (Figs. 11a-c).

| | |
|---|---|
| L *[cm]* | 1 |
| H *[cm]* | 4 |
| Width *[cm]* | 0.1 |
| Height of the protein chamber h *[cm]* | 1.948 |
| $D_{lys}$ *[cm]* | $10^{-6}$ |
| $D_{NaCl}$ *[cm]* | $10^{-5}$ |
| ν *[cm]* | 8.63 $10^{-3}$ |
| $\rho_c$ *[cm]* | 1.2 |
| $\beta_{lys}$ *[(g/cm3) -1]* | 0.3 |
| $\beta_{NaCl}$ *[(g/cm3) -1]* | 0.6 |
| $C_{lys(o)}$ *[g/cm3]* | 4 $10^{-2}$ |
| $C_{NaCl(o)}$ *[g/cm3]* | 14 $10^{-2}$ |
| Sc | 8630 |
| Rav | $10^4$ |
| Computational points along x | 60 |
| Computational points along y | 190 |

*Table I: data used for numerical simulation*

The distribution of crystals at the end of the process (Fig.12) is more regular with respect to the worst condition. However the effect of g-jitter cannot be considered negligible. The symmetry of the solid pattern is distorted with respect to gellified conditions. For this reason, this analysis clearly shows that no "ideal" conditions exist in the case of Liesegang pattern formation phenomena under the effect of sinusoidal acceleration. While in the case of typical non-isothermal experiments under microgravity conditions, investigators can minimize g-jitter effects orienting their fluid-cell up to make the sinusoidal acceleration parallel to the imposed temperature difference, in the case of experiments dealing with periodic precipitation, this is not possible. In fact, no preferential direction of the concentration gradients can be found or fixed "a priori". Even if the nucleation phenomena can be (roughly) schematized for the present case as a wave migrating along a fixed direction (the y axis), however, due to the nucleation phenomena, concentration gradients oriented both in the axial and transversal directions arise (i.e. along x and y) leading locally to the onset of convection.

Note that in the worst case the depletion zone created around each growing crystal is distorted by two different effects: the "large scale" flow due to solutal g-jitter and the motion of the crystal itself. In the ideal case, since the presence of vortex cells is strictly confined to the zones around the nucleation front (it is a "local" phenomenon), more stable depletion zones occur. These aspect are crucial for the quality of the crystals. According to the previously highlighted critical role played by the stability of the depletion zone, better crystals are expected to be obtained in the ideal case (even if the spatial distribution of crystal is not symmetric as for the worst case). A quantitative investigation of these aspects requires the detailed simulation of the interface attachment kinetics and surface morphology evolution of each crystal. These aspects are out the scope of the present work and are delayed to forthcoming analyses dealing with the very detailed investigation of the "local" evolution.

Figs. 13 and 14 compare the solid particle size and density of particles distributions under diffusive regime and g-jitter conditions. In the latter environment the number of crystals tends to be reduced with respect to the case of gellified protein solution. This effect is related to the presence of convection due to g-jitter that strengthens protein mixing and therefore promotes further growth after nucleation.

## 5. Conclusions

The complex dynamics of the crystallization process of lysozyme have been investigated under diffusive conditions (on ground crystal sedimentation prevented by the use of agarose gel in the protein solution) and microgravity (protein solution free of gel and crystal motion allowed). For the latter case a sinusoidal high frequency acceleration has been taken into account corresponding to typical oscillatory disturbances (Lab Ergometer condition) occurring on the International Space Station. The analysis has required the application of already existing mathematical models and appropriate numerical methods to handle the complex phenomena related to protein nucleation and further precipitation or resolution according to the protein concentration distribution and the supersaturation limit. Further to these models, novel numerical techniques and methods have been introduced in the case of g-jitter to investigate the motion of the crystals due to the disturbance time-averaged velocity field and the interaction of this motion with the concentration field. For the first case under investigation (protein solution gellified), the results have shown that the phenomenon exhibits a wave-like behaviour. The crystal formation results modulated in time and in space, due to the non-linear interplay among transport, crystal nucleation and growth and Liesegang patterns appear. In the case of g-jitter acceleration perpendicular to the imposed salt and protein concentration gradients (worst case), the results show that convection cells arise due to density gradients associated to salt diffusion and protein depletion. These vortices have the classical Gershuni configuration, i.e. two couples of counter-rotating vortex cells. Solid particles are transported towards the gel interface near the walls and in opposite direction around the mid-section. At each instant the line of separation between the two couples of convection cells corresponds (approximately) to the position of the nucleation front. As time passes the nucleation front and the line of separation migrate increasing their distance from the gel interface. The depletion zones (whose stability is crucial for the quality of the crystals) created around each growing seed are distorted by the large scale flow and by the motion of the crystals.

If the g-jitter acceleration is applied to the protein chamber parallel to the imposed salt and protein concentration gradients ("ideal case"), the presence of vortex cells is strictly confined to the zones where new nucleation and/or further precipitation occurs (i.e. multicellular convective structures located around the nucleation front). The region affected by convection migrates with the nucleation front whereas the remaining part of the protein chamber is free of convection. Accordingly improvement of the quality of the crystals is expected to be obtained in this case. For both cases however, the effect of g-jitter on the pattern of crystals cannot be considered negligible. The symmetry of the pattern is distorted with respect to gellified conditions. The present analysis may support the optimization of growth techniques under the effect of periodic accelerations providing for instance information about the relative direction of g-jitter and imposed concentration gradients that should lead to better crystals for diffraction analyses. This contribution appears as the first attempt to analyze in detail these behaviours. The prediction of the models here presented may be verified in microgravity imposing controlled vibrations to a crystal growth reactor. For this reason future experimental investigation of these topics is needed.

## 6. Acknowledgements

The present work has been supported by the European Space Agency (ESA) and the Italian Space Agency (ASI). The authors would like to thank the Referees for the constructive comments, Dr. Chiara Piccolo (from MARS) for the useful information provided on experimentally observed phenomena and on the configuration of typical experiments. The authors also undebted Dr. Dario Castagnolo (from MARS) and Professor J.M. Garcìa-Ruiz (Granada University) for the precious suggestions

## 7. References

*[1] Ramachandran N., Baugher Ch. R., Naumann R.J.*, "Modeling flows and transport in protein crystal growth", Microgravity sci. technol. Vol. VIII/3, p. 170 (1995)

*[2] Qi J., Wakayama N. I.,* "Solute convection during the whole process of protein crystal growth", J. Cryst. Growth, Vol. 219, p. 465, (2000).

*[3] Otàlora F., Novella M. L., Gavira J. A., Thomas B. R., Garcìa-Ruiz J.M.,* 'Experimental evidence for the stability of the depletion zone around a growing protein crystal under microgravity', Acta Crys., Vol. D57, p. 412, (2001).

*[4] Pusey M. L., Snyder R. S., Naumann R.,* 'Protein crystal growth: growth kinetics for tetragonal lysozyme crystals', Journal of Biological Chemistry, Vol. 261 No. 14, p. 6524, (1986).

*[5] Monaco A., Rosenberger F.,* 'Growth and etching kinetics of tetragonal lysozyme', J. Cryst. Growth, Vol. 129, p. 465, (1993).

*[6] Kuznetsov Yu G., Malkin A. J., Greenwood A., McPherson A.,* 'Interferometric studies of growth kinetics and surface morphology in macromolecular crystal growth: canavalin, thaumatin and turnip yellow mosaic virus', Journal of structural biology, Vol. 114, p. 184, (1995).

*[7] Coriell S. R., Chernov A.A., Murray B.T., McFadden G.B.,* "Step bunching: generalized kinetics", Journal of Crystal Growth Vol. 183, p. 669 , (1998).

*[8] Otàlora F., Garcìa-Ruiz J.M.,* "Crystal growth studies in microgravity with the APCF: Computer simulation and transport dynamics", Journal of Crystal Growth, Vol. 182, p. 141, (1987).

*[9] Henisch H.K., Garcìa-Ruiz J.M.,* "Crystal growth in gels and Liesegang ring formation: Crystallization criteria and successive precipitation", Journal of Crystal Growth, Vol. 75, p. 203, (1986).

*[10] Henisch H. K.,* "Periodic Precipitation: a microcomputer analysis of transport and reaction processes in diffusion media with software development", Pergamon Press, (1991).

*[11] Galkin O., Vekilov P. G.,* "Direct determination of the nucleation rates of protein crystals", J. Phys. Chem. B, Vol. 103, p. 10965, (1999).

*[12] Monti R., Langbein D., Favier J.J.,* "Influence of residual accelerations on fluid physics and material science experiments", in Fluid and material Science

in Space, H.U. Walter ed., (1987).
*[13] Mc Fadden G.B., Coriell S.R.,* "Solutal convection during directional solidification", AIAA paper 88-3635-CP, (1988).
*[14] Schneider S., Straub J.,* "Influence of the Prandtl number on laminar natural convection in a cylinder caused by g-jitter", J. Crystal Growth, Vol. 46, p. 125, (1989).
*[15] Alexander J.I.D.,* "Low gravity experiment sensitivity to residual acceleration: a review", Microgravity Sci. and Tech., Vol. 3, p. 52, (1990).
*[16] Ramachandran N.,* "G-jitter convection in enclosures", 9th International Heat Transfer Conference, paper 8-MC-03, Jerusalem, Israel (August 1990)
*[17] Monti R., Savino R.,* "The basis and the recent developments of OMA and its applications to microgravity". Microgravity Quarterly Vol. 5, No.1, p. 13, (1994).
*[18] Monti R., Savino R.,* "A new approach to g-level tolerability for Fluid and Material Science experiments". Acta Astronautica Vol. 37, p. 313, (1994).
*[19] Monti R., Savino R.,* "Influence of g-jitter on fluid physics experimentation on-board the International Space Station". ESA SP-385, p. 215, (1996).
*[20] Monti R., Savino R.,* "Microgravity experiment acceleration tolerability on space orbiting laboratories", Journal of Spacecraft and Rockets Vol. 33, No.5, p. 707, (1996).
*[21] Savino R., Monti R.,* "Convection induced by residual-g and g-jitters in diffusion experiments", Int. J. Heat and Mass Transfer Vol.42, p. 111, (1999).
[22] Gershuni G.Z., Zhukhovitskii E.M., Yurkov Yu. S., "Vibrational thermal convection in a rectangular cavity", Izv. Akad. Nauk SSSR Mekh. Zhidk. Gaza Vol. 4, p. 94, (1982).
*[23] Lappa M.;* "Strategies for parallelizing the three-dimensional Navier-Stokes equations on the Cray T3E "; Science and Supercomputing at CINECA, M. Voli Editor, Bologna, p. 326, (1997).
*[24] Piccolo C., Lappa M., Tortora A., Castagnolo D., Carotenuto L.,* "Non-linear behaviour of lysozyme crystallization", Physica A: Statistical Mechanics and its Applications Vol. 314, No. 1-4, p. 636, (2002).
*[25] Lappa M., Castagnolo D., Carotenuto L.,* "Sensitivity of the non-linear dynamics of lysozyme 'Liesegang Rings' to small asymmetries", Physica A: Statistical Mechanics and its Applications Vol. 314, No. 1-4, p. 623, (2002).